

Preparation of a ternary Pd–Rh–P amorphous alloy and its catalytic performance in selective hydrogenation of alkynes†

Cite this: *Catal. Sci. Technol.*, 2014, 4, 1920

Received 18th March 2014,
Accepted 2nd May 2014

Mengrui Ren, Changming Li, Jiale Chen, Min Wei* and Shuxian Shi*

DOI: 10.1039/c4cy00338a

www.rsc.org/catalysis

Palladium–rhodium–phosphorus amorphous alloy nanoparticles (~5.2 nm) were prepared via a facile one-pot synthesis method, exhibiting excellent catalytic behaviour in selective hydrogenation of alkynes under mild conditions.

Alloy catalysts have recently attracted considerable attention in heterogeneous catalysis^{1–3} because the incorporation of a second metal is an effective approach for tailoring electronic and geometric properties and thus optimizing the catalytic performance. Especially, amorphous alloys,^{4,5} as a relatively young class of materials with short-range order and long-range disorder, have shown promising catalytic performance in many hydrogenation reactions (e.g., selective hydrogenation of diene, selective hydrogenation of benzene,⁶ hydrogenation of sulfolene⁷ and hydrosulphurization of dibenzothiophene⁸). In addition, Yamashita *et al.*⁹ reported that amorphous alloys have much higher catalytic activity than alloys in the crystallized state, resulting from the active site number and the electronic state of surface metals. However, previous studies mainly focused on monometallic alloys with non-metallic elements (e.g., Ni–B amorphous alloy⁶), and there are very few reports^{7,8} on bimetallic amorphous catalysts. The reason can be explained as follows: two completely fused metal elements in a phase diagram (e.g., Pd and Pt^{10,11}) are apt to form a crystallized but not amorphous alloy while in the case of two incompletely- or non-fused metal elements (e.g., Pd and Rh), it's rather difficult to obtain amorphous alloys based on conventional methods. Taking into account the unique merits of amorphous alloys, fabricating bimetallic amorphous alloys with promising behaviour in heterogeneous catalysis is of vital importance and remains a great challenge.

Herein, we report the synthesis of monodispersed PdRhP amorphous alloy nanoparticles (NPs) via co-reduction of Pd(acac)₂

and Rh(acac)₃, employing trioctylphosphine (TOP) as the stabilizer. The XRD pattern and HRTEM image confirm the amorphous structure feature of the alloy NPs with a mean size of 5.2 ± 0.4 nm, and the aberration-corrected scanning transmission electron microscopy with energy dispersive X-ray mapping-scan (STEM-EDS) further demonstrates the uniform distribution of Pd, Rh and P elements in each amorphous particle. The catalytic performance of PdRhP amorphous alloy NPs was investigated in the chemoselective hydrogenation of various alkynes. Interestingly, high selectivity toward various alkenes was observed in a few hours with a high conversion (up to 100%) under quite mild reaction conditions (atmospheric pressure and 35 °C) which is superior to their single counterparts, showing promising applications in catalysis.

Uniform alloy NPs with an average size of 5.2 ± 0.4 nm were successfully synthesized in high yield (the detailed experimental procedure is described in the ESI†) and are arranged regularly just like a decorative pattern (Fig. 1a). No distinct reflection corresponding to crystalline phases can be observed in the XRD pattern aside from one broad peak at

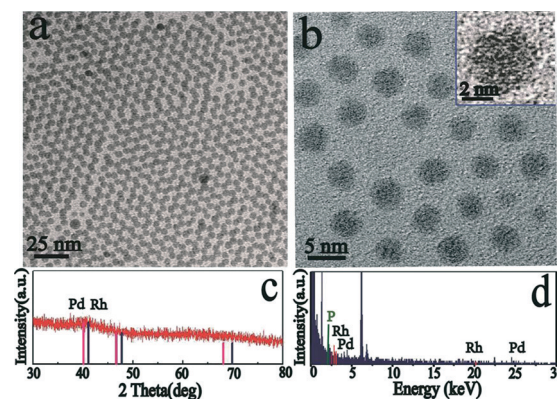


Fig. 1 (a) The TEM image of the alloy NPs, (b) the HRTEM image of the amorphous alloy NPs (inset: enlarged HRTEM image), (c) the XRD pattern and (d) the EDX spectrum of the alloy NPs.

State Key Laboratory of Chemical Resource Engineering, Beijing University of Chemical Technology, Beijing, PR China. E-mail: weimin@mail.buct.edu.cn, shisx@mail.buct.edu.cn; Fax: +86 10 64425385

† Electronic supplementary information (ESI) available. See DOI: 10.1039/c4cy00338a

$2\theta \sim 45^\circ$ (Fig. 1c), which is rather different from that of single crystalline Pd or Rh NPs (Fig. S1†). This indicates the formation of an amorphous alloy structure. Moreover, despite the signals of Pd and Rh elements both being captured (Fig. 1d), no lattice fringe image can be detected for the alloy NPs *via* the HRTEM technology (Fig. 1b, inset). Both the typical features above confirm the amorphous state of the alloy NPs.

In order to study the distribution of these two metal elements, high-angle annular dark-field scanning transmission electron microscopy (HAADF-STEM) was used to carry out further analysis (Fig. 2a). The energy dispersive X-ray (EDX) mapping-scan recorded through the single nanoparticle in the red square frame (Fig. 2a) shows a similar element distribution of Pd and Rh (Fig. 2b). The line-scan spectra of Pd and Rh which were collected through the center of an individual nanoparticle (marked by the red line in Fig. 2a) also show rather similar behavior of Pd and Rh, demonstrating homogeneous dispersion of these two species in an individual particle. This was further verified by detecting more than ten nanoparticles (Fig. 2c).

Moreover, it is worth noting that a strong P element signal was also detected in the NPs (Fig. 1d), suggesting that P may participate in the formation of the amorphous alloy structure. We further performed elemental analysis of the amorphous alloy and the results are listed in Table S1†. The results demonstrate the existence of P with a molar percentage of 27%. This was further confirmed by the HAADF-STEM-EDS technique (Fig. S2†), and a uniform inter-distribution of Pd, Rh, P can be observed in all of the amorphous nanoparticles by the EDX-mapping scan. Fig. S3† displays the XRD patterns of alloy materials synthesized with various P/metal ratios, and it was found that the amorphous phase can only form at a high level of nominal P/metal ratio (14/1, Fig. S3A†). Therefore, it can be concluded that the as-synthesized amorphous alloy is a ternary system (denoted as Pd₃₄Rh₃₉P₂₇).

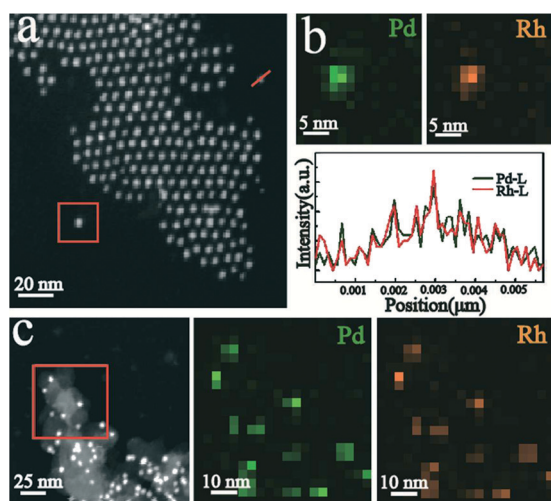


Fig. 2 (a) The HAADF-STEM image of the alloy NPs, (b) the EDX mapping image and line scanning results of an individual alloy particle, and (c) the mapping image of a few alloy NPs supported on SiO₂. Green: Pd-L; yellow: Rh-L.

The semihydrogenation of alkynes plays a key role in industry because alkyne impurities in the olefin feedstocks will lead to the deactivation of the polymerization catalyst.^{12,13}

Pd is regarded as the best active component in this reaction. As a result, the selective hydrogenation of alkynes was employed as the model reaction to evaluate the catalytic performance of the amorphous alloy. For comparison, pristine Rh and pristine Pd NPs with close sizes (~ 5.2 nm) were prepared by regulating the temperature and the amount of the capping agent using the same method (Fig. 3). Commercial Rh/C and Pd/C were also employed as contrast catalysts. The concentration of each catalyst was determined so as to ensure the same noble metal content of all the catalyst samples. The hydrogenation of a model alkyne, phenylacetylene, was carried out at quite low temperature (35 °C) and atmospheric pressure. Fig. 4a shows the composition variation of the reaction mixture over the alloy amorphous catalyst at different points in time. The content of phenylacetylene decreased gradually in the whole reaction time range (3 h), while the styrene content increased rapidly at first and reached a maximum (100% conversion with 82% selectivity) at 2.5 h, followed by a sharp decrease from 2.5 to 3.0 h (Fig. 4a), exhibiting the well-known behaviour of consecutive reactions. The content of ethylbenzene, the complete hydrogenation product, exhibits a slow increase (0–2.5 h) and a fast enhancement (2.5–3.0 h). The best yield (82%) of styrene can be achieved at 2.5 h (Fig. 4b).

In contrast, single Pd NPs and Pd/C show rather high catalytic activity: phenylacetylene completely transforms to ethylbenzene quickly in less than one hour and a half (Fig. 4c). The Pd NPs show a slightly higher selectivity than Pd/C at various conversion levels, but both of them have lower selectivity than Pd₃₄Rh₃₉P₂₇ NPs (Fig. 4d). For Rh catalysts, both the Rh NPs and Rh/C samples display rather low conversion for the whole reaction duration (0–3.0 h); moreover, the selectivity dramatically decreased with the increase of conversion (0–20%). For comparison, the Lindlar Pd–Pb/CaCO₃ catalyst was also evaluated (Fig. 4d), displaying a maximum olefin yield of 86.7%, close to that of the previous report.¹⁴ The Pd₃₄Rh₃₉P₂₇ catalyst in this work shows a close maximum yield to that of the Lindlar Pd–Pb/CaCO₃ one, indicating a

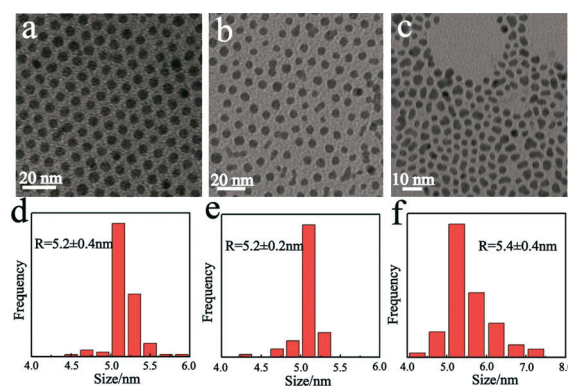


Fig. 3 TEM images of (a) Pd–Rh–P, (b) Rh, and (c) Pd NPs with the corresponding size distributions.

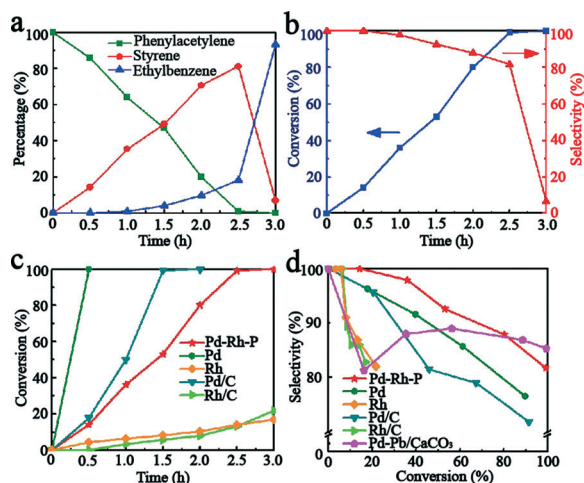


Fig. 4 (a) Product distribution of phenylacetylene hydrogenation as a function of reaction time over the bimetallic amorphous catalyst. (b) The conversion of phenylacetylene and selectivity for styrene in the reaction time range 0–3.0 h. (c) The phenylacetylene conversion as a function of time over various catalysts, with a metal amount of 0.16 μmol . (d) The styrene selectivity vs. phenylacetylene conversion over various catalysts with the following metal contents: $\text{Pd}_{34}\text{Rh}_{39}\text{P}_{27}$: 0.16 μmol ; Pd: 0.08 μmol ; Rh: 0.16 μmol ; Pd/C: 0.08 μmol ; Rh/C: 0.16 μmol ; and Pd–Pb/CaCO₃: 0.08 μmol .

similar bimetallic reaction mechanism for the improved catalytic performance.^{15,16} Therefore, it is concluded that the PdRhP amorphous alloy exhibits significantly superior activity and selectivity to their single counterparts (pristine Pd or Rh catalyst).

Since some previous studies^{17–19} showed that the high catalytic activity of nanoparticles might be due to molecular species leaching from the nanoparticles, we conducted a filtration test to investigate this issue. The hydrogenation of phenylacetylene catalyzed by alloy NPs was terminated after 1 h at a conversion of 81% (Fig. S4†), then the H₂ pressure was released and the nanoparticles were removed by centrifugation. Subsequently, the filtrate was placed into the flask to restart the reaction under the same conditions for one hour.

No obvious change in the mixture composition was observed except for a rather slight increase in the phenylacetylene conversion which might be due to the residual catalyst in the filtrate. This suggests that the alloy NPs are responsible for the catalytic activity. The cycle ability of alloy NPs was also explored by employing the selective hydrogenation of phenylacetylene. The catalyst was separated by centrifugation, washed and reused without further treatment. After five cycles, the conversion of phenylacetylene still remained 100% and no obvious change in the product composition was found (Fig. S5†). From the viewpoint of practical applications, supporting nano-catalysts on a carrier is highly significant for improving stability, separation and recycling.²⁰ This is under investigation in our lab.

Furthermore, the ternary amorphous alloy also exhibits excellent catalytic performance in selective hydrogenation of other alkynes, and the results are given in Table 1. For 4-nitroethynylbenzene hydrogenation, a high selectivity of 94.7% (at 44.4% conversion) for the olefin was obtained over the $\text{Pd}_{34}\text{Rh}_{39}\text{P}_{27}$ alloy, which was maintained at a high level (99.2% selectivity) even at 100% conversion. However, a relatively low selectivity or quite low activity was observed over single Pd (81.5% selectivity at 45.9% conversion) or Rh catalyst, respectively. In the case of 4-bromostyrene hydrogenation, the $\text{Pd}_{34}\text{Rh}_{39}\text{P}_{27}$ NPs display rather satisfactory catalytic behavior both at low and high conversions (95.5% selectivity at 38.5% conversion; 91.9% selectivity at 100% conversion) compared with the monometallic Pd or Rh catalyst. Hydrogenation of tolane was also investigated. The $\text{Pd}_{34}\text{Rh}_{39}\text{P}_{27}$ (72.9% selectivity at 40.1% conversion) and pristine Pd (69.4% selectivity at 51.7% conversion) catalysts revealed rather similar catalytic behavior in this reaction while the Rh/C sample shows the highest selectivity for (*Z*)-stilbene (78.3%) but at rather low conversion (25.2%). These results demonstrate that $\text{Pd}_{34}\text{Rh}_{39}\text{P}_{27}$ displays greatly enhanced catalytic performance in selective hydrogenation of various alkynes compared with the pristine Pd or Rh catalyst.

Based on the results above, it can be seen that the pristine Pd catalyst shows limited selectivity, in accordance with the

Table 1 Selective hydrogenation reaction of various alkynes

Substrates							
Catalyst	Time (h)	Con. (%)	Sel. ^a (%)	Con. (%)	Sel. ^b (%)	Con. (%)	Sel. ^c (%)
$\text{Pd}_{34}\text{Rh}_{39}\text{P}_{27}$	4	100	99.2	100	91.9	99.3	54.9 <i>cis</i>
	2.5	78.6	98.6	67.2	93.3	73.5	77.9 <i>cis</i>
	1.5	44.4	94.7	38.5	95.5	40.1	72.9 <i>cis</i>
Pd	4	100	0	100	84.7	99.4	57.1 <i>cis</i>
	2.5	86.3	73.7	83.1	80.5	82.8	61.8 <i>cis</i>
	1.5	45.9	81.5	39.9	87.2	51.7	69.4 <i>cis</i>
Pd/C	4	100	0	62.5	88.9	99.4	55.2 <i>cis</i>
	2.5	76.9	83.9	48.7	95.7	76.5	66.4 <i>cis</i>
	1.5	38.7	87.3	26.8	93.2	47.7	74.2 <i>cis</i>
Rh/C	Rh/C	0	0	12.6	81.4	25.2	78.3 <i>cis</i>

Reaction conditions: dioxane (1 ml), 1 bar H₂, 35 °C. ^a Selectivity for 1-ethenyl-4-nitrobenzene. ^b Selectivity for 4-bromostyrene. ^c Selectivity for (*Z*)-stilbene.

previous reports.^{21,22} This can be possibly attributed to the formation of a hydride phase which is active in over-hydrogenation reactions.²³ The employment of a second element is the main strategy to improve performance of Pd catalysts (e.g., Pd-Ga,²⁴ Pd-Cu,²⁵ Pd-Ni¹² and Pd-Si²⁶). The presence of other metals or metalloids would modify the geometric effect and electron density of Pd atom, influencing the adsorption behavior of reactants and intermediates.²⁷

In this work, Rh and P elements in the PdRhP amorphous alloy may function in a similar way (e.g., the geometric and electronic modification effect of Rh and P elements^{12,24,28}) to improve the hydrogenation selectivity for alkynes. On the other hand, the inherent nature of the amorphous alloy may also have a unique influence on the enhanced selectivity. From a theoretical point of view, the metalloid element in an amorphous alloy could change the coordination environment of an active metal (e.g., in the NiB system²⁹), and the short-range order between neighboring metal atoms would influence the adsorption of reactants.³⁰ Therefore, the improved catalytic performance of PdRhP can be attributed to the intrinsic nature of the amorphous alloy with a modified geometric/electronic structure, which will be studied in our future work.

In summary, this work provides a facile method for the preparation of ternary PdRhP amorphous alloy NPs with a uniform particle size. The combination of Pd and Rh with the presence of P shows excellent catalytic performance in hydrogenation of several alkynes under mild reaction conditions compared with the pristine Rh or Pd catalyst. This approach can be extended to other amorphous bimetallic alloys with superior catalytic behavior and potential applications in industrial hydrogenation reactions.

Acknowledgements

This work was supported by the 973 Program (grant no. 2011CBA00504), the National Natural Science Foundation of China (NSFC), the Scientific Fund from Beijing Municipal Commission of Education (20111001002) and the Fundamental Research Funds for the Central Universities (ZD 1303). M. Wei particularly appreciates the financial aid from the China National Funds for Distinguished Young Scientists of the NSFC.

Notes and references

- P. Rodriguez, F. D. Tichelaar, M. T. M. Koper and A. I. Yanson, *J. Am. Chem. Soc.*, 2011, **133**, 17626–17629.
- S. Zafeirotas, S. Piccinin and D. Teschner, *Catal. Sci. Technol.*, 2012, **2**, 1787–1801.
- E. C. Corbos, P. R. Ellis, J. Cookson, V. Briois, T. I. Hyde, G. Sankar and P. T. Bishop, *Catal. Sci. Technol.*, 2013, **3**, 2934–2943.
- Z. Jiang, H. Yang, Z. Wei, Z. Xie, W. Zhong and S. Wei, *Appl. Catal., A*, 2005, **279**, 165–171.
- Y. Chen, B. Liaw and S. Chiang, *Appl. Catal., A*, 2005, **284**, 97–104.
- (a) M. Shapaan, A. Bárdos, L. K. Varga and J. Lendvai, *Mater. Sci. Eng., A*, 2004, **366**, 6–9; (b) H. E. Schone, H. C. Hoke and A. Johnson, *Mater. Sci. Eng.*, 1988, **97**, 431–435; (c) Y. Ma, W. Li, M. Zhang, Y. Zhou and K. Tao, *Appl. Catal., A*, 2003, **243**, 215–223; (d) H. Li, D. Chu, J. Liu, M. Qiao, W. Dai and H. Li, *Adv. Synth. Catal.*, 2008, **350**, 829–836.
- Y. Ma, W. Li, M. Zhang, Y. Zhou and K. Tao, *Appl. Catal., A*, 2003, **243**, 215–223.
- L. Song, W. Li, G. Wang, M. Zhang and K. Tao, *Catal. Today*, 2007, **125**, 137–142.
- H. Yamashita, M. Yoshikawa, T. Funabiki and S. Yoshida, *J. Chem. Soc., Faraday Trans. 1*, 1986, **82**, 1771–1780.
- H. Zhang, M. Jin, H. Liu, J. Wang, M. J. Kim, D. Yang, Z. Xie, J. Liu and Y. Xia, *ACS Nano*, 2011, **5**, 8212–8222.
- X. Huang, Y. Li, Y. Li, H. Zhou, X. Duan and Y. Huang, *Nano Lett.*, 2012, **12**, 4265–4270.
- S. Domínguez-Domínguez, Á. Berenguer-Murcia, D. Cazorla-Amorós and Á. Linares-Solano, *J. Catal.*, 2006, **243**, 74–81.
- F. M. McKenna, L. Mantarosie, R. P. K. Wells, C. Hardacre and J. A. Anderson, *Catal. Sci. Technol.*, 2012, **2**, 632–638.
- T. A. Nijhuis, G. van Koten and J. A. Moulijn, *Appl. Catal., A*, 2003, **238**, 259–271.
- P. W. Albers, K. Möbus, C. D. Frost and S. F. Parker, *J. Phys. Chem. C*, 2011, **115**, 24485–24493.
- F. M. McKenna, R. P. K. Wells and J. A. Anderson, *Chem. Commun.*, 2011, **47**, 2351–2353.
- L. D. Pachón and G. Rothenberg, *Appl. Organomet. Chem.*, 2008, **22**, 288–299.
- J. S. Chen, A. N. Vasiliev, A. P. Panarello and J. G. Khinast, *Appl. Catal., A*, 2007, **325**, 76–86.
- S. S. Soomro, F. L. Ansari, K. Chatziapostolou and K. Köhler, *J. Catal.*, 2010, **273**, 138–146.
- (a) M. Comotti, W. C. Li, B. Spliethoff and F. Schüth, *J. Am. Chem. Soc.*, 2006, **128**, 917–924; (b) L. N. Protasova, E. V. Rebrov, K. L. Choy, S. Y. Pung, V. Engels, M. Cabaj, A. E. H. Wheatley and J. C. Schouten, *Catal. Sci. Technol.*, 2011, **1**, 768–777; (c) N. Lopez, J. K. Nørskov, T. V. W. Janssens, A. Carlsson, A. Puig-Molina, B. S. Clausen and J.-D. Grunwaldt, *J. Catal.*, 2004, **225**, 86–94; (d) S. Domínguez-Domínguez, Á. Berenguer-Murcia, Á. Linares-Solano and D. Cazorla-Amorós, *J. Catal.*, 2008, **257**, 87–95.
- C. A. Hamilton, S. D. Jackson, G. J. Kelly, R. Spence and D. Bruin, *Appl. Catal., A*, 2002, **237**, 201–209.
- J. Osswald, R. Giedigkeit, R. E. Jentoft, M. Armbrüster, F. Girgsdies, K. Kovnir, T. Ressler, Y. Grin and R. Schlögl, *J. Catal.*, 2008, **258**, 210–218.
- (a) D. Teschner, J. Borsodi, A. Wootsch, Z. Révay, M. Hävecker, A. Knop-Gericke, S. D. Jackson and R. Schlögl, *Science*, 2008, **320**, 86–89; (b) N. López and C. Vargas-Fuentes, *Chem. Commun.*, 2012, **48**, 1379–1391; (c) M. García-Mota, B. Bridier, J. Pérez-Ramírez and N. López, *J. Catal.*, 2010, **273**, 92–102.
- G. Wowsnick, D. Teschner, M. Armbrüster, I. Kasatkin, F. Girgsdies, Y. Grin, R. Schlögl and M. Behrens, *J. Catal.*, 2014, **309**, 221–230.

- 25 M. B. Boucher, B. Zugic, G. Cladaras, J. Kammert, M. D. Marcinkowski, T. J. Lawton, E. C. H. Sykes and M. Flytzani-Stephanopoulos, *Phys. Chem. Chem. Phys.*, 2013, **15**, 12187–12196.
- 26 R. Tschan, R. Wandeler, M. S. Schneider, M. M. Schubert and A. Baiker, *J. Catal.*, 2001, **204**, 219–229.
- 27 D. Mei, M. Neurock and C. M. Smith, *J. Catal.*, 2009, **268**, 181–195.
- 28 (a) A. M. Alexander and J. S. J. Hargreaves, *Chem. Soc. Rev.*, 2010, **39**, 4388–4401; (b) B. Rajesh, N. Sasirekha and Y. W. Chen, *J. Mol. Catal. A: Chem.*, 2007, **275**, 174–182; (c) S. Carenco, A. Leyva-Pérez, P. Concepción, C. Boissière, N. Mézailles, C. Sanchez and A. Corma, *Nano Today*, 2012, **7**, 21–28.
- 29 H. Li, J. Zhang and H. Li, *Catal. Commun.*, 2007, **8**, 2212–2216.
- 30 (a) M. Crespo-Quesada, J. M. Andanson, A. Yarulin, B. Lim, Y. Xia and L. Kiwi-Minsker, *Langmuir*, 2011, **27**, 7909–7916; (b) A. M. Alexander and J. S. J. Hargreaves, *Chem. Soc. Rev.*, 2010, **39**, 4388–4401; (c) S. Yoshida, H. Yamashita, T. Funabiki and T. Yonezawa, *J. Chem. Soc., Faraday Trans. 1*, 1984, **80**, 1435–1446; (d) H. Yamashita, M. Yoshikawa, T. Funabiki and S. Yoshida, *J. Chem. Soc., Faraday Trans. 1*, 1985, **81**, 2485–2493.